Journal of Solid State Chemistry **159,** 321–327 (2001)
doi:10.1006/jssc.2001.9161, available online at http://www.idealibrary.com on IDEAL®

High-Temperature Reactions of Metal Triangles: The Influence of Counterion, Ligand, and Metal on the Structure Observed

Robert A. Coxall,* Andrew Parkin,* Simon Parsons,* Andrew A. Smith,† Grigore A. Timco,‡ and Richard E. P. Winpenny†,[1]

*Department of Chemistry, University of Edinburgh, West Mains Road, Edinburgh, United Kingdom; †Department of Chemistry, University of Manchester, Oxford Road, Manchester, United Kingdom; and ‡Institute of Chemistry, Moldovan Academy of Sciences, Kishinev MD-2028, Moldova

Received March 20, 2001; accepted March 21, 2001

IN DEDICATION TO THE LATE PROFESSOR OLIVIER KAHN FOR HIS PIONEERING CONTRIBUTIONS TO THE FIELD OF MOLECULAR MAGNETISM

A series of oxo-centered metal carboxylate triangles have been heated to 200–400°C under a stream of N_2. The products of this treatment depend on the metal, carboxylate, and counterion present. Heating $[Cr_3O(O_2CC_6H_4Cl)_6(H_2O)_3][NO_3]$to 200°C gives a compound that crystallizes as $[Cr(OH)(O_2CC_6H_4Cl)_2]_8[Cr_3O(O_2CC_6H_4Cl)_6]_2[O_2CC_6H_4Cl]$, indicating incomplete dehydration of $[Cr_3O(O_2CC_6H_4Cl)_6(H_2O)_3][NO_3]$ at this temperature. For $[Cr_3O(O_2CCMe_3)_6][O_2CCMe_3]$ heating to 400°C gives a new salt containing the hexanuclear cages $[Cr_6O_2(OH)_2(O_2CCMe_3)_{11}]$ $[Cr_6O_4(O_2CCMe_3)_{11}]$. For $[Mn_3O(O_2CPh)_6(NC_5H_5)_2(H_2O)]$ a reduction of the metal occurs and a polymeric complex $[Mn_4(O_2CPh)_8(EtOH)_6]_n$ can be crystallized from EtOH. © 2001 Academic Press

Key Words: **chromium; manganese; cage complexes; X-ray crystallography.**

INTRODUCTION

One of the major goals of scientists studying "molecular magnetism" is to discover new routes to molecular objects with new magnetic properties (1). We have been investigating transformations of coordination complexes at 200–400°C in the solid state (2–4). While such temperatures are moderate in solid state chemistry, they are abnormally high for metal-organic chemistry. We have previously found that oxo-centered chromium carboxylate triangles oligomerize at these temperatures, giving a range of cages depending on the carboxylate used. For example, using pivalate (O_2CCMe_3) gave a dodecanuclear cage $[Cr_{12}O_9(OH)_3(O_2CCMe_3)_{15}]$, which has an $S = 6$ spin ground state (3). Here we report investigations of others aspects of this reaction.

[1]To whom correspondence should be addressed. E-mail: richard.winpenny@man.ac.uk.

EXPERIMENTAL

All reagents, metal salts, and ligands were used as obtained from Aldrich.

$[Mn_3O(O_2CPh)_6(py)_2(H_2O)]$ was synthesized by a literature procedure (5). Analytical data were obtained on a Perkin–Elmer 2400 Elemental Analyzer by the University of Edinburgh Microanalytical Service. Electrospray mass spectra were obtained on a sample dissolved in $MeOH/CH_2Cl_2$ 1:10 using a Micromass Platform Mass Spectrometer.

Preparation of Compounds

$[Cr_3O(O_2CC_6H_4Cl)_6(H_2O)_3](NO_3)$. KOH (105.0 mmol, 5.89 g) was dissolved in H_2O (125 ml) and $ClC_6H_4CO_2H$ (105.0 mmol, 16.44 g) added. The mixture was heated to 80°C with stirring and CH_3OH (30 ml) added to aid dissolution of $ClC_6H_4CO_2H$. $Cr(NO_3)_3{\cdot}9H_2O$ (50.0 mmol, 20.00 g) was then added to this solution, resulting in a light blue precipitate forming. This precipitate was filtered off and dried in vacuo. The yield of this crude product was 19.293 g (94.77%).

$[Cr_3O(O_2CC_6H_4Cl)_6(EtOH)_2(H_2O)]_2[Cr_8(OH)_8(O_2CC_6H_4Cl)_{16}][O_2CC_6H_4Cl]$ **1**. $[Cr_3O(O_2CC_6H_4Cl)_6(H_2O)_3][NO_3]$ (1.712 g, 1.4 mmol) was heated from room temperature to 200°C in a tube furnace under a continuous stream of N_2. After 5 min. at 200°C, the reaction was allowed to cool. The dark green solid that resulted was extracted with EtOH (50 ml), the solution filtered and allowed to stand at room temperature. After repeated filtration of the solution, dichromic blue/purple crystals of **1** grew after 4 months in 2% yield. Insufficient material was formed for elemental analysis.

$[Cr_3O(O_2CC(CH_3)_3)_6(H_2O)_3](O_2CC(CH_3)_3)$. $(CH_3)_3CCO_2H$ (100.0 mmol, 10·21 g) was heated to 100°C with

0022-4596/01 $35.00

TABLE 1
Experimental Data for the X-Ray Diffraction Studies of Compounds1–3

Compound	1	2	3
Formula	$C_{112}H_{72}Cl_{16}Cr_8O_{48}{\cdot}2C_{46}H_{38}Cl_6Cr_3O_{16}{\cdot}1.3C_7H_5ClO_2{\cdot}2NO_3{\cdot}19$ EtOH·2.1 H_2O	$C_{55}H_{100}Cr_6O_{26}{\cdot}3C_2H_3N$	$C_{72}H_{82}Mn_4O_{24}{\cdot}$ EtOH
M	6712.5	1611.5	1551.1
Crystal system	Monoclinic	monoclinic	triclinic
Space group	$P\,2/c$	$P\,2_1/n$	$P-1$
a (Å)	27.323(3)	17.871(15)	12.841(8)
b (Å)	17.499(2)	19.524(16)	13.398(7)
c (Å)	35.991(4)	24.253(19)	13.416(8)
α (°)	90	90	66.92(3)
β (°)	104.506(3)	93.109(18)	67.97(2)
γ (°)	90	90	72.47(2)
U (Å^3)	16660(4)	8450(12)	1935.9(19)
T (K)	150.0(2)	150.0(2)	220.0(2)
Z	2	4	1[c]
D_c (g cm^{-3})	1.338	1.267	1.330
Crystal shape and color	Dichromic purple/ blue rod	Green needle	Colorless rod
Crystal size (mm)	$0.17\times0.10\times0.09$	$0.21\times0.06\times0.06$	$0.38\times0.08\times0.08$
μ (mm^{-1})	0.749	0.812	0.710
Unique data	34,036	17,100	3603
Unique data with $F_o>4\sigma(F_o)$	11,649	8233	1245
Parameters	1352	784	458
Restraints	63	0	72
Max. Δ/σ ratio	0.001	0.053	0.001
$R1$, $wR2$[a]	0.0862, 0.2682	0.0654, 0.1728	0.0924, 0.2210
Weighting scheme[b] (w^{-1})	$\sigma^2(F_o^2)+(0.1199P)^2$	$\sigma^2(F_o^2)+(0.0812P)^2$	$\sigma^2(F_o^2)+(0.0597P)^2$
Goodness of fit	0.944	0.921	0.960
Largest residuals (e Å^{-3})	+0.852, −0.647	+0.638, −0.270	+0.406, −0.405

[a] $R1$ based on observed data, $wR2$ on all unique data.
[b] $P=1/3[\max(F_o^2{\cdot}0)+2F_o]$.
[c] The compound is polymeric: z is quoted for the repeat unit.

stirring and $Cr(NO_3)_3{\cdot}9H_2O$ (25.0 mmol, 10.0 g) added. This mixture was refluxed for an hour and the temperature was then raised to 150°C for 15 min., or until the evolution of NO_2 ceased. The resulting mixture was cooled to room temperature. The product was dissolved in 4:1 EtOH/H_2O and heated to 80°C, the solution was filtered hot, and green crystals formed on cooling. The yield was 3.407 g (43.8%).

$[Cr_6O_2(OH)_2(O_2CCMe_3)_{11}][Cr_6O_4(O_2CCMe_3)_{11}]$ **2.** $[Cr_3O(O_2CCMe_3)_6(H_2O)_3][O_2CCMe_3]$ (2.56 g, 2.74 mmol) was heated from room temperature to 300°C in a tube furnace under a continuous stream of N_2. After 30 min. at 300°C, the reaction was allowed to cool. The dark green solid which resulted was extracted with MeCN (30 ml), the solution filtered and allowed to stand at room temperature. Dark green crystals of **2** grew after 2 months in 65% yield. Elemental analysis: found, C, 42.9%; H, 6.7%. Calculated for **2**, C, 44.4%; H, 6.8%.

$[Mn_4(O_2CPh)_8(EtOH)_6]$ **3.** $[Mn_3O(O_2CPh)_6(py)_2(H_2O)]$ (5) (1.53 g, 1.41 mmol) was heated from room temperature to 300°C in a tube furnace under a continuous stream of N_2. After 5 min at 300°C, the reaction was allowed to cool. The dark brown solid that resulted was extracted with EtOH (25 ml), the solution filtered and allowed to stand at room temperature. Very light beige crystals of **3** grew after 20 days in 60% yield. Elemental analysis: found, C, 54.5%, H; 4.9%. Calculated for **3**, C, 55.4%; H, 5.2%.

Crystallography. Crystal data and data collection and refinement parameters for compounds **1**–**3** are given in Table 1, selected bond lengths and angles in Tables 2–6.

Data collection and processing. Data for **1** and **2** were collected on a Bruker Smart APEX CCD area detector and for **3** on a Stoe Stadi-4 four-circle diffractometer. Both diffractometers were equipped with an Oxford Cryosystems low-temperature device (6), and used graphite-monochromated MoK_α radiation, with ϕ–ω scans for **1** and **2**, and ω–θ scans for **3**. Data were corrected for Lorentz and

TABLE 2
Selected Bond Lengths (Å) for 1

	Octanuclear wheel		
Cr(1)–O(12W)	1.926(4)	Cr(1)–O(21)	1.965(5)
Cr(1)–O(11)	1.973(40)	Cr(2)–O(12W)	1.912(4)
Cr(2)–O(22)	1.962(5)	Cr(2)–O(12)	1.985(4)
Cr(2)–(23W)	1.919(4)	Cr(2)–O(42)	1.973(4)
Cr(2)–O(32)	1.982(5)	Cr(3)–O(23W)	1.916(4)
Cr(3)–O(33)	1.954(5)	Cr(3)–O(43)	1.978(4)
Cr(3)–O(34W)	1.924(4)	Cr(3)–O(63)	1.968(5)
Cr(3)–O(53)	1.982(4)	Cr(4)–O(34W)	1.920(4)
Cr(4)–O(54)	1.982(4)	Cr(4)–O(64)	1.949(15)
Cr(4)–O(45W)	1.923(4)	Cr(4)–O(74)	1.954(5)
Cr(4)–O(84)	1.960(4)	Cr(5)–O(45W)	1.926(4)
Cr(5)–O(85)	1.981(4)	Cr(5)–O(75)	1.963(5)
	Oxo-centered triangle		
Cr(1T)–O(123)	1.876(5)	Cr(1T)–O(1B)	1.952(7)
Cr(1T)–O(1A)	1.954(6)	Cr(1T)–O(1E)	1.968(6)
Cr(1T)–O(1F)	1.973(7)	Cr(1T)–O(1T)	2.103(7)
Cr(2T)–O(123)	1.913(5)	Cr(2T)–O(2D)	1.949(5)
Cr(2T)–O(2B)	1.955(6)	Cr(2T)–O(2C)	1.960(5)
Cr(2T)–O(2A)	1.971(6)	Cr(2T)–O(2T)	2.049(5)
Cr(3T)–O(123)	1.918(5)	Cr(3T)–O(3C)	1.944(5)
Cr(3T)–O(3F)	1.958(6)	Cr(3T)–O(3E)	1.963(6)
Cr(3T)–O(3D)	1.973(5)	Cr(3T)–O(3T)	2.040(5)

TABLE 3
Selected Bond Angles (°) for 1

Octanuclear wheel			
O(12W)–Cr(1)–O(12W)′	88.1(2)	O(12W)–Cr(1)–O(21)′	90.34(17)
O(12W)–Cr(1)–O(21)	93.38(18)	O(21)–Cr(1)–O(21)′	174.8(2)
O(12W)–Cr(1)–O(11)′	179.4(2)	O(12W)–Cr(1)–O(11)	91.42(17)
O(21)–Cr(1)–O(11)	90.15(18)	O(21)–Cr(1)–O(11)′	86.16(18)
O(11)–Cr(1)–O(11)′	89.0(2)	O(12W)–Cr(2)–O(23W)	90.29(16)
O(12W)–Cr(2)–O(22)	92.66(19)	O(23W)–Cr(2)–O(22)	88.17(18)
O(12W)–Cr(2)–O(42)	174.49(17)	O(22)–Cr(2)–O(42)	87.61(19)
O(23W)–Cr(2)–O(42)	95.22(17)	O(12W)–Cr(2)–O(32)	91.47(19)
O(22)–Cr(2)–O(32)	175.23(19)	O(23W)–Cr(2)–O(32)	89.41(18)
O(42)–Cr(2)–O(32)	88.5(2)	O(12W)–Cr(2)–O(12)	89.63(17)
O(22)–Cr(2)–O(12)	91.96(19)	O(23W)–Cr(2)–O(12)	179.8(2)
O(42)–Cr(2)–O(12)	84.86(17)	O(32)–Cr(2)–O(12)	90.5(2)
O(23W)–Cr(3)–O(34W)	90.07(16)	O(23W)–Cr(3)–O(33)	88.59(18)
O(34W)–Cr(3)–O(33)	91.57(18)	O(23W)–Cr(3)–O(63)	89.94(19)
O(33)–Cr(3)–O(63)	178.5(2)	O(34W)–Cr(3)–O(63)	88.62(18)
O(23W)–Cr(3)–O(43)	93.09(16)	O(33)–Cr(3)–O(43)	91.6(2)
O(34W)–Cr(3)–O(43)	174.00(17)	O(63)–Cr(3)–O(43)	88.3(2)
O(23W)–Cr(3)–O(53)	175.03(17)	O(33)–Cr(3)–O(53)	88.7(2)
O(34W)–Cr(3)–O(53)	92.17(16)	O(63)–Cr(3)–O(53)	92.8(2)
O(43)–Cr(3)–O(53)	82.83(17)	O(34W)–Cr(4)–O(45W)	91.81(16)
O(34W)–Cr(4)–O(64)	90.23(18)	O(45W)–Cr(4)–O(64)	89.6(2)
O(34W)–Cr(4)–O(74)	88.82(18)	O(64)–Cr(4)–O(74)	178.1(2)
O(45W)–Cr(4)–O(74)	92.10(19)	O(34W)–Cr(4)–O(84)	176.99(19)
O(64)–Cr(4)–O(84)	87.9(2)	O(45W)–Cr(4)–O(84)	90.50(18)
O(74)–Cr(4)–O(84)	93.0(2)	O(34W)–Cr(4)–O(54)	93.51(17)
O(64)–Cr(4)–O(54)	90.2(2)	O(45W)–Cr(4)–O(54)	174.67(17)
O(74)–Cr(4)–O(54)	88.2(2)	O(54)–Cr(4)–O(84)	84.17(18)
O(45W)–Cr(5)–O(45W)	86.6(2)	O(45W)–Cr(5)–O(75)	92.93(18)
O(45W)–Cr(5)–O(75)	89.86(18)	O(45W)–Cr(5)–O(85)	92.74(17)
O(75)–Cr(5)–O(75)′	176.2(2)	O(45W)–Cr(5)–O(85)′	179.32(19)
O(75)–Cr(5)–O(85)	90.31(19)	O(85)–Cr(5)–O(85)′	87.9(2)
O(75)–Cr(5)–O(85)′	86.93(18)		
Oxo-centered triangle			
O(123)–Cr(1T)–O(1B)	93.2(2)	O(123)–Cr(1T)–O(1A)	96.4(2)
O(1B)–Cr(1T)–O(1A)	96.4(2)	O(123)–Cr(1T)–O(1E)	94.6(2)
O(1A)–Cr(1T)–O(1E)	87.9(2)	O(1B)–Cr(1T)–O(1E)	172.3(3)
O(123)–Cr(1T)–O(1F)	94.2(2)	O(1A)–Cr(1T)–O(1F)	169.3(3)
O(1B)–Cr(1T)–O(1F)	87.3(3)	O(1E)–Cr(1T)–O(1F)	92.4(2)
O(123)–Cr(1T)–O(1T)	178.6(3)	O(1A)–Cr(1T)–O(1T)	85.0(3)
O(1B)–Cr(1T)–O(1T)	86.9(3)	O(1E)–Cr(1T)–O(1T)	85.4(3)
O(1F)–Cr(1T)–O(1T)	84.4(3)	O(123)–Cr(2T)–O(2D)	97.2(2)
O(123)–Cr(2T)–O(2B)	94.2(2)	O(2D)–Cr(2T)–O(2B)	89.1(2)
O(123)–Cr(2T)–O(2C)	92.6(2)	O(2B)–Cr(2T)–O(2C)	173.0(2)
O(2D)–Cr(2T)–O(2C)	92.0(2)	O(123)–Cr(2T)–O(2A)	96.6(2)
O(2B)–Cr(2T)–O(2A)	90.0(2)	O(2D)–Cr(2T)–O(2A)	166.1(2)
O(2C)–Cr(2T)–O(2A)	87.3(2)	O(123)–Cr(2T)–O(2T)	178.7(2)
O(2B)–Cr(2T)–O(2T)	84.6(2)	O(2D)–Cr(2T)–O(2T)	83.1(2)
O(2C)–Cr(2T)–O(2T)	88.8(2)	O(2A)–Cr(2T)–O(2T)	83.0(2)
O(123)–Cr(3T)–O(3C)	92.9(2)	O(123)–Cr(3T)–O(3F)	95.0(2)
O(3C)–Cr(3T)–O(3F)	171.8(2)	O(123)–Cr(3T)–O(3E)	94.4(2)
O(3F)–Cr(3T)–O(3E)	90.9(2)	O(3C)–Cr(3T)–O(3E)	86.5(2)
O(123)–Cr(3T)–O(3D)	95.3(2)	O(3F)–Cr(3T)–O(3D)	88.2(2)
O(3C)–Cr(3T)–O(3D)	93.1(2)	O(3E)–Cr(3T)–O(3D)	170.3(2)
O(123)–Cr(3T)–O(3T)	178.6(2)	O(3F)–Cr(3T)–O(3T)	86.3(2)
O(3C)–Cr(3T)–O(3T)	85.7(2)	O(3E)–Cr(3T)–O(3T)	85.5(2)
O(3D)–Cr(3T)–O(3T)	84.8(2)		

TABLE 4
Selected Bond Lengths (Å) for 2

Cr(1)–O(1D)	1.943(3)	Cr(1)–O(123)	1.950(3)
Cr(1)–O(124)	1.962(3)	Cr(1)–O(1A)	1.993(3)
Cr(1)–O(1C)	1.995(3)	Cr(1)–O(1)	2.036(3)
Cr(2)–O(124)	1.941(3)	Cr(2)–O(1G)	1.950(3)
Cr(2)–O(123)	1.956(3)	Cr(2)–O(1B)	0.1981(3)
Cr(2)–O(2A)	2.001(3)	Cr(2)–O(2)	2.028(3)
Cr(3)–O(123)	1.951(3)	Cr(3)–O(1H)	1.961(3)
Cr(3)–O(1E)	1.968(4)	Cr(3)–O(1)	1.970(3)
Cr(3)–O(2C)	1.976(3)	Cr(3)–O(2)	2.042(3)
Cr(4)–O(124)	1.954(3)	Cr(4)–O(1F)	1.960(3)
Cr(4)–O(2)	1.977(3)	Cr(4)–O(1I)	1.977(3)
Cr(4)–O(2B)	1.983(3)	Cr(4)–O(1)	2.031(3)
Cr(5)–O(1)	1.960(3)	Cr(5)–O(2D)	1.964(3)
Cr(5)–O(2F)	1.968(4)	Cr(5)–O(2E)	1.976(4)
Cr(5)–O(2J)	2.012(3)	Cr(5)–O(1J)	2.047(4)
Cr(6)–O(2)	1.956(3)	Cr(6)–O(2I)	1.959(4)
Cr(6)–O(2H)	1.967(4)	Cr(6)–O(2G)	1.974(3)
Cr(6)–O(2K)	2.006(3)	Cr(6)–O(1K)	2.043(4)

polarization factors. Absorption corrections were applied to all data, using Sadabs (7) for **1** and **2**, and by Gaussian integration following refinement of the crystal shape and dimensions against a set of ψ-scans for **3**.

Structure analysis and refinement. Structures **1** and **3** were solved by direct methods using SHELXS-97 (8), while **2** was solved by the heavy atom method using DIRDIF (9). All structures were completed by iterative cycles of ΔF syntheses and full-matrix least-squares refinement against F^2 (SHELXL-97) (8). All non-H atoms within the metal complexes were refined anisotropically. H atoms were included in calculated positions, and were assigned isotropic thermal parameters ($U(\mathrm{H}) = 1.5\ U_{\mathrm{eq}}(\mathrm{C})$ for methyl and methylene H atoms; $U(\mathrm{H}) = 1.2\ U_{\mathrm{eq}}(\mathrm{C})$ for aromatic protons). Methyl groups in **3** were treated as rigid rotating groups. For **1** and **2** the lattice solvent was treated in the manner described by van der Sluis and Spek (10) (1080 e/cell for **1** and 238 e/cell for **2**). In the case of **1** this density was assumed to comprise the nitrate counterions and solvent (EtOH) of crystallization; in **2** it was taken to be MeCN of crystallization. Densities, values of $F(000)$, and absorption coefficients have been calculated to take this into account.

Additional material available from the Cambridge Crystallographic Data Centre comprises atom coordinates, thermal parameters, and remaining bond lengths and angles.

RESULTS AND DISCUSSION

In previous studies of the thermally induced oligomerization of oxo-centered chromium carboxylate triangles, we have shown that the resulting product can be influenced by the choice of carboxylate (2–4). We have proposed (4) that this control is related to whether water or carboxylic acid or both are eliminated on heating. Thus, reaction of $[Cr_3O(O_2CPh)_6(H_2O)_2(OH)]$ at 400°C produces a tetracapped heterocubane $[Cr_8O_4(O_2CPh)_{16}]$ **4**, which involves loss of water only, while reaction of $[Cr_3O(O_2CCMe_3)_6(H_2O)_3][NO_3]$ leads to a centered pentacapped trigonal prism, $[Cr_{12}O_9(OH)_3(O_2CCMe_3)_{15}]$ **5**, which involves loss of carboxylic acid. Here we discuss structural results for a number of other variations.

Use of *para*-chlorobenzoate as the carboxylate within the oxo-centered triangle gives a reactivity similar to that of

TABLE 5
Selected Bond Lengths (°) for 2

O(1D)–Cr(1)–O(123)	176.36(12)	O(1D)–Cr(1)–O(124)	96.37(14)
O(123)–Cr(1)–O(124)	83.73(13)	O(1D)–Cr(1)–O(1A)	89.55(12)
O(124)–Cr(1)–O(1A)	89.26(12)	O(123)–Cr(1)–O(1A)	86.81(11)
O(1D)–Cr(1)–O(1C)	91.87(15)	O(124)–Cr(1)–O(1C)	169.52(13)
O(123)–Cr(1)–O(1C)	88.46(14)	O(1A)–Cr(1)–O(1C)	97.28(13)
O(1D)–Cr(1)–O(1)	97.68(12)	O(124)–Cr(1)–O(1)	79.54(12)
O(123)–Cr(1)–O(1)	85.92(11)	O(1A)–Cr(1)–O(1)	167.25(12)
O(1C)–Cr(1)–O(1)	92.98(12)	O(124)–Cr(2)–O(1G)	176.45(12)
O(124)–Cr(2)–O(123)	84.10(13)	O(1G)–Cr(2)–O(123)	96.32(14)
O(124)–Cr(2)–O(1B)	88.35(14)	O(123)–Cr(2)–O(1B)	169.77(13)
O(1G)–Cr(2)–O(1B)	91.65(15)	O(124)–Cr(2)–O(2A)	87.53(12)
O(123)–Cr(2)–O(2A)	89.11(12)	O(1G)–Cr(2)–O(2A)	88.96(12)
O(1B)–Cr(2)–O(2A)	97.46(13)	O(124)–Cr(2)–O(2)	86.15(11)
O(123)–Cr(2)–O(2)	79.80(11)	O(1G)–Cr(2)–O(2)	97.39(12)
O(1B)–Cr(2)–O(2)	92.86(12)	O(2A)–Cr(2)–O(2)	167.73(12)
O(123)–Cr(3)–O(1H)	91.72(12)	O(123)–Cr(3)–O(1E)	179.60(14)
O(1H)–Cr(3)–O(1E)	87.92(13)	O(123)–Cr(3)–O(1)	87.72(12)
O(1E)–Cr(3)–O(1)	92.65(13)	O(1H)–Cr(3)–O(1)	179.43(13)
O(123)–Cr(3)–O(2C)	89.44(12)	O(1E)–Cr(3)–O(2C)	90.37(14)
O(1H)–Cr(3)–O(2C)	87.61(14)	O(1)–Cr(3)–O(2C)	92.31(14)
O(123)–Cr(3)–O(2)	79.56(11)	O(1E)–Cr(3)–O(2)	90.37(14)
O(1H)–Cr(3)–O(2)	95.52(14)	O(1)–Cr(3)–O(2)	92.31(14)
O(2C)–Cr(3)–O(2)	168.63(13)	O(124)–Cr(4)–O(1F)	91.83(13)
O(124)–Cr(4)–O(2)	87.25(12)	O(1F)–Cr(4)–O(2)	179.07(13)
O(124)–Cr(4)–O(1I)	178.94(13)	O(2)–Cr(4)–O(1I)	92.13(13)
O(1F)–Cr(4)–O(1I)	88.79(13)	O(124)–Cr(4)–O(2B)	89.14(13)
O(2)–Cr(4)–O(2B)	91.79(14)	O(1F)–Cr(4)–O(2B)	88.08(14)
O(1I)–Cr(4)–O(2B)	90.02(14)	O(124)–Cr(4)–O(1)	79.86(12)
O(2)–Cr(4)–O(1)	84.57(13)	O(1F)–Cr(4)–O(1)	95.39(14)
O(1I)–Cr(4)–O(1)	100.94(13)	O(2B)–Cr(4)–O(1)	168.56(13)
O(1)–Cr(5)–O(2D)	94.67(14)	O(1)–Cr(5)–O(2F)	88.27(16)
O(2D)–Cr(5)–O(2F)	88.27(16)	O(1)–Cr(5)–O(2E)	92.80(14)
O(2F)–Cr(5)–O(2E)	93.27(16)	O(2D)–Cr(5)–O(2E)	172.15(14)
O(1)–Cr(5)–O(2J)	172.34(16)	O(2F)–Cr(5)–O(2J)	91.07(16)
O(2D)–Cr(5)–O(2J)	86.18(15)	O(2E)–Cr(5)–O(2J)	86.09(15)
O(1)–Cr(5)–O(1J)	107.61(14)	O(2F)–Cr(5)–O(1J)	155.72(14)
O(2D)–Cr(5)–O(1J)	87.55(15)	O(2E)–Cr(5)–O(1J)	87.90(16)
O(2J)–Cr(5)–O(1J)	64.79(15)	O(2)–Cr(6)–O(2I)	93.13(14)
O(2)–Cr(6)–O(2H)	97.35(14)	O(2I)–Cr(6)–O(2H)	92.79(17)
O(2)–Cr(6)–O(2G)	94.90(13)	O(2H)–Cr(6)–O(2G)	88.95(15)
O(2I)–Cr(6)–O(2G)	171.51(14)	O(2)–Cr(6)–O(2K)	171.71(17)
O(2H)–Cr(6)–O(2K)	90.91(17)	O(2I)–Cr(6)–O(2K)	85.82(15)
O(2G)–Cr(6)–O(2K)	85.84(14)	O(2)–Cr(6)–O(1K)	107.37(15)
O(2H)–Cr(6)–O(1K)	155.25(15)	O(2I)–Cr(6)–O(1K)	87.05(17)
O(2G)–Cr(6)–O(1K)	87.90(15)	O(2K)–Cr(6)–O(1K)	64.38(17)

TABLE 6
Selected Bond Lengths (Å) and Angles (°) for 3

Mn(1)–O(1)	2.153(13)	Mn(1)–O(5)	2.177(13)
Mn(1)–O(3)	2.194(12)	Mn(2)–O(7)	2.048(12)
Mn(2)–O(2)′	2.073(13)	Mn(2)–O(4)	2.109(13)
Mn(2)–O(9)	2.165(15)	Mn(2)–O(6)	2.289(14)
Mn(2)–O(5)	2.322(11)	Mn(3)–O(8)	2.104(15)
Mn(3)–O(10)	2.159(14)	Mn(3)–O(11)	2.179(13)
O(1)–Mn(1)–O(5)	91.8(5)	O(1)–Mn(1)–O(3)	85.6(5)
O(3)–Mn(1)–O(5)	93.0(4)	O(7)–Mn(2)–O(2)′	107.7(6)
O(7)–Mn(2)–O(4)	91.2(6)	O(2)′–Mn(2)–O(4)	92.8(5)
O(7)–Mn(2)–O(9)	92.1(6)	O(2)′–Mn(2)–O(9)	86.8(5)
O(4)–Mn(2)–O(9)	176.7(6)	O(7)–Mn(2)–O(6)	97.8(5)
O(2)′–Mn(2)–O(6)	154.4(5)	O(4)–Mn(2)–O(6)	88.6(5)
O(9)–Mn(2)–O(6)	90.4(5)	O(7)–Mn(2)–O(5)	154.9(5)
O(2)′–Mn(2)–O(5)	97.0(5)	O(4)–Mn(2)–O(5)	91.7(4)
O(9)–Mn(2)–O(5)	85.2(5)	O(6)–Mn(2)–O(5)	57.4(4)
O(8)–Mn(3)–O(10)	92.6(6)	O(8)–Mn(3)–O(11)	86.4(5)
O(10)–Mn(3)–O(11)	93.6(5)		

benzoate itself. Heating $[Cr_3O(O_2CC_6H_4Cl)_6(H_2O)_3][NO_3]$ to 200°C gives blue/purple crystals, which structural analysis reveals to contain two cages. The first is a oxo-centered triangle similar to the starting material (Fig. 1), where the oxo-centered triangular array of Cr atoms each has a Cr … Cr vector bridges by a *para*-chlorobenzoate ligand, and the three terminal sites on the Cr centers are occupied by one water and two EtOH molecules. The second molecule is an octanuclear wheel, $[Cr_8(OH)_8(O_2CC_6H_4Cl)_{16}]$ (Fig. 2), which lies on a crystallographic twofold axis passing through Cr(1) and Cr(5). Within the cyclic structure each Cr … Cr vector is bridged by one hydroxide and two carboxylate ligands. Similar Cr wheels have been reported with benzoate as the bridging carboxylate (2), and a related wheel has been found where the single-atom bridge is fluoride and the carboxylate is pivalate (11). A molecule of *para*-chlorobenzoate is found H-bonded to the OH protons of the wheel. Cr–O bond lengths lie in the expected range for this metal and oxidation state. The Cr … Cr contacts within the triangle vary from 3.292(3) to 3.299(3) Å, while those within the wheel vary from 3.391(3) to 3.414(3) Å.

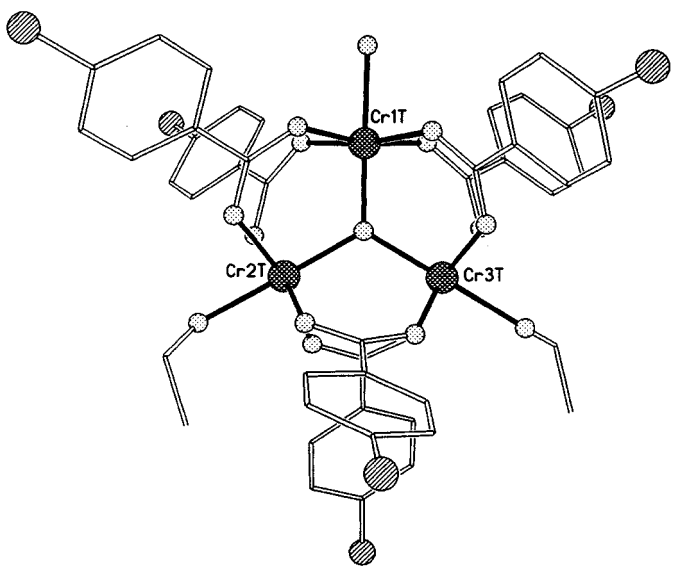

FIG. 1. The structure of the oxo-centered triangle in **1**. O atoms, dotted spheres; C atoms, cross-hatched spheres. Top-right to bottom-left hatched spheres; Cl atoms.

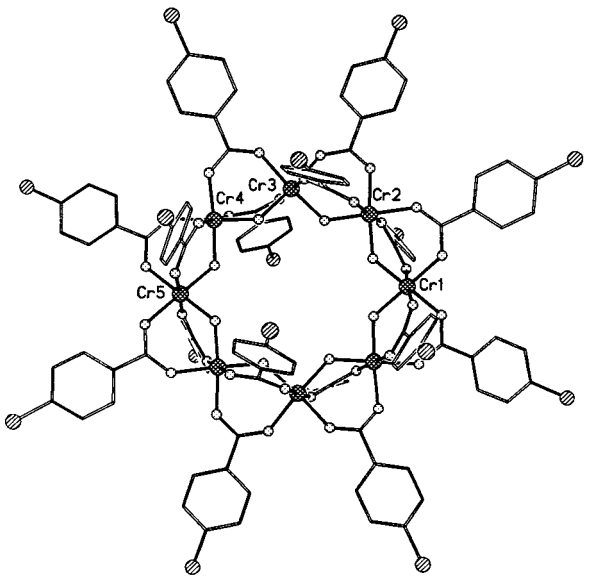

FIG. 2. The structure of the octanuclear chromium wheel in **1**. Shading is as described in the legend to Fig. 1.

As the octanuclear wheel lies on a twofold axis there are two trimers for each octamer within the crystal lattice, giving a stoichiometry of $[Cr_3O(O_2CC_6H_4Cl)_6(EtOH)_2(H_2O)]_2[Cr_8(OH)_8(O_2CC_6H_4Cl)_{16}][O_2CC_6H_4Cl]$ **1**. This creates an apparent complication, as there are two cations for every anion. This can be explained in two ways. Firstly, it is not certain that the coordinated water within the trinuclear units is always water, and not hydroxide. Secondly, there is a very large amount of disordered "solvent" in the crystal lattice (approx. 1080 electrons per unit cell), which could not be refined but which may contain hydroxide or nitrate counterions. There is no question of chromium being present in any oxidation state other than $+3$, and therefore the apparent absence of an anion does not create any ambiguities in interpreting the coordination chemistry.

The formation of the octanuclear wheel is a dehydration of the oxo-centered triangle. The fact that the triangle co-crystallizes with the wheel indicates that this reaction is incomplete at 200°. The yield of **1** is poor at present. Heating to higher temperatures (≥ 300°C) causes greater dehydration, and formation of a species that we believe to be $[Cr_8O_4(O_2CC_6H_4Cl)_{16}]$ (12), but which we have not yet been able to crystallize. Similar reactivity is shown by the benzoate trimer. We hope that extended heating times, and possibly the presence of a dehydrating agent may allow the wheels to be synthesized in higher yield.

Investigation of the influence of the anion led us to examine the thermally induced oligomerization of $[Cr_3O(O_2CCMe_3)_6(H_2O)_3][O_2CCMe_3]$. Heating this salt to 300°C, followed by recrystallization from MeCN, gives a hexanuclear cage $[Cr_6O_4(O_2CCMe_3)_{11}]$ (Fig. 3). The structure consists of a Cr_4O_4 heterocubane, with two additional Cr atoms attached to two of the four O atoms of the cube. This is related to **4**, where all four O atoms bridge to further Cr centers. Each Cr ... Cr vector is further bridged by a 1,3-bridging pivalate. Cr–O bond lengths lie in the expected range for this metal and oxidation state. The Cr ... Cr contacts within the heterocubane vary from 2.833(2) to 3.061(2) Å, while the contacts between Cr atoms within the cubane and Cr(5) and Cr(6) are longer, varying from 3.417(2) to 3.509(2) Å.

There are three chemically distinct Cr sites within the cage. The first pair of sites, Cr(1) and Cr(2), are each bound to one μ_4- and two μ_3-oxygen atoms within the heterocubane, one O atom from a pivalate ligand that spans the top face of the cube, bridging Cr(1) and Cr(2), one O atom from a pivalate that bridges to another vertex of the heterocubane, and a final pivalate oxygen where the carboxylate bridges to a capping Cr center. The second pair, Cr(3) and Cr(4), are the remaining vertices of the cubane, and are each bound to one μ_3- and two μ_4-oxygen atoms, an O atom that forms part of a pivalate that bridges to Cr(1) or Cr(2) respectively, and two O atoms from pivalates that bridge to the capping chromium sites. The third pair, Cr(5) and Cr(6), cap the cubane, and bind to one μ_4-oxygen atom from the cubane, three O atoms from pivalates that bridge to the cube, and two O donors from a chelating pivalate ligand.

As for **1**, there appears to be a problem with charge balance, which cannot be resolved by X-ray diffraction. However, electrospray mass spectrometry is extremely informative. In the negative ion spectrum the only strong multiplet is found centered at m/z 1488, while in the positive ion spectrum the multiplet is found at m/z 1490. These two multiplets are due to $[Cr_6O_4(O_2CCMe_3)_{11}]^-$ and

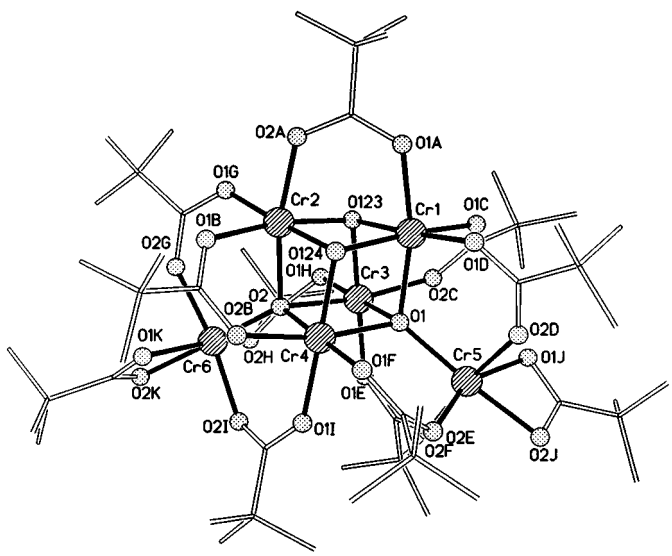

FIG. 3. The structure of the hexanuclear bicapped-heterocubane in **2**. O atoms, dotted spheres; C atoms, hatched spheres.

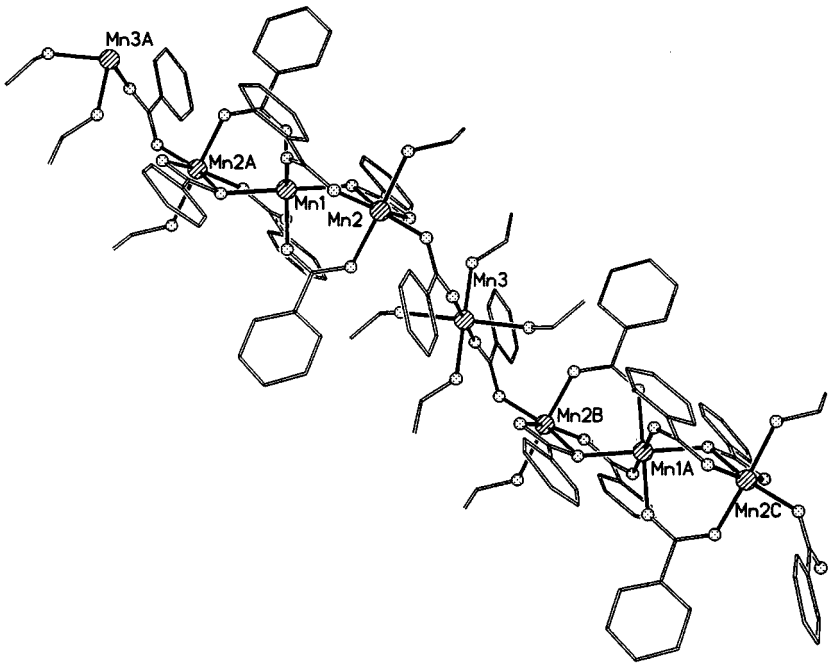

FIG. 4. A section of the one-dimensional polymer in **3**. O atoms, dotted spheres; C atoms, hatched spheres.

$[Cr_6O_2(OH)_2(O_2CCMe_3)_{11}]^+$ respectively, and therefore we believe the crystal contains species where the μ_3-oxygen atoms [O(123) and O(124) in Fig. 3] are deprotonated and species where both μ_3-O atoms are protonated, and **2** should be written $[Cr_6O_2(OH)_2(O_2CCMe_3)_{11}]$ $[Cr_6O_4(O_2CCMe_3)_{11}]$. We cannot exclude the possibility that the neutral species $[Cr_6O_3(OH)(O_2CCMe_3)_{11}]$ is also present in the lattice.

Therefore $[Cr_3O(O_2CCMe_3)_6(H_2O)_3][O_2CCMe_3]$ appears to react very differently to $[Cr_3O(O_2CCMe_3)_6$ $(H_2O)_3][NO_3]$ (3). With the nitrate counterion, pivalic acid was lost on heating at 400°C, to give **5**, while with a pivalate counterion the salt **2** is formed. The pivalate:Cr ratio is markedly lower in **5** (15:12) than in **2** (22:12), and this may be due to the additional pivalate present as counterion in the starting material for **2**. Compound **2** is also an additional member of a growing family of chromium heterocubane cages, which now contain hexa-, octa- (2), and dodecanuclear (4) members.

Varying the metal present in the initial oxo-centered triangle has more dramatic results. Heating the mixed-valent compound $[Mn_3O(O_2CPh)_6(py)_2(H_2O)]$ (7) to 300°C under N_2 leads to an oxidation state change from Mn(III) to Mn(II), presumably accompanied by loss of O_2. Cyrstallization of the resulting solid from EtOH gives a one-dimensional polymeric complex $[Mn_4(O_2CPh)_8(EtOH)_6]$ **3** (Fig. 4). The structure is best considered as linear trinuclear $[Mn_3(O_2CPh)_6(EtOH)_2]$ cages linked through *trans*-$[Mn(O_2CPh)_2(EtOH)_4]$ mononuclear units. Within the trinuclear "bricks," each Mn … Mn vector is bridged by two 1,3-bridging benzoates and the O atom of a third benzoate that acts as a chelating ligand to the external Mn site of the trinuclear block. The central Mn site [Mn(1)] is bound exclusively to benzoate O atoms acting in a monodentate fashion to this site. The external Mn site [Mn(2)] is bound to two O atoms from a chelating benzoate, two O atoms from benzoates that bridge to Mn(1), one terminal EtOH molecule, and a benzoate that bridges to the mononuclear fragment containing Mn(3). The Mn(3) site is bound to four EtOH molecules and two bridging benzoates, with the bridging ligands arranged in a *trans* geometry with respect to each other. The Mn–O bond lengths are unexceptional.

The formation of **3**, while clearly dependent on the crystallization solvent, does suggest that the reactivity of the oxo-centered triangles will prove markedly different for redox active metal centers than for Cr(III). The results reported here indicate that a very large body of polynuclear cage complexes can be made by these routes, and raise the possibility of influencing the complexes formed by choice of ligand, anion, and metal, and probably also temperature, reaction time, and heating rate.

ACKNOWLEDGMENT

We thank the EPSRC(UK) for funding for a diffractometer, an electrospray mass spectrometer, a Fellowship (to R.A.C), and a studentship (to A.A.S.).

REFERENCES

1. O. Kahn, "Molecular Magnetism." VCH, New York, 1994.
2. I. M. Atkinson, C. Benelli, M. Murrie, S. Parsons, and R. E. P. Winpenny, *Chem. Commun.* 285–286 (1999).
3. F. E. Mabbs, E. J. L. McInnes, M. Murrie, S. Parsons, C. C. Wilson, and R. E. P. Winpenny, *Chem. Commun.* 643–644 (1999).
4. S. Parsons, A. A. Smith, and R. E. P. Winpenny, *Chem. Commun.* 579–580 (2000).
5. J. B. Vincent, H.-R. Change, K. Folting, J. C. Huffman, G. Christou, and D. N. Hendrickson, *J. Am. Chem. Soc.* **109,** 5703–5711 (1987).
6. J. Cosier and A. M. Glazer, *J. Appl. Crystallogr.* **19,** 105 (1986).
7. SADABS: Area-Detector Absorption Correction. Siemens Industrial Automation, Inc., Madison, WI, 1996.
8. G. M. Sheldrick, SHELX97, Programs for Crystal Structure Analysis (Release 97-2). Institüt für Anorganische Chemie, Universität Göttingen, Germany, 1998.
9. P. T. Beurskens, G. Beurskens, W. P. Bosman, R. de Gelder, S. Garcia-Granda, R. O. Gould, R. Israel, and J. M. M. Smits, DIRDIF96 program system. Crystallography Laboratory, University of Nijmegen, The Netherlands, 1996.
10. SQUEEZE P. van der Sluis and A. L. Spek, *Acta Crystallogr. Sect. A* **46,** 194–201 (1990).
11. N. V. Gerbeleu, Yu. T. Struchkov, G. A. Timco, A. S. Batsanov, K. M. Indrichan, and G. A. Popovich, *Dokl. Akad. Nauk. SSSR* **313,** 1459–1463 (1990).
12. A. A. Smith and R. E. P. Winpenny, unpublished results.